








## Article

# Kufahrite, PtPb, a new mineral from Ledyanoy Creek placer, Galmoenan ultramafic complex, Koryak Highlands, Russia

Evgeniy G. Sidorov<sup>1</sup>† , Anton V. Kutuyev<sup>1\*</sup> , Elena S. Zhitova<sup>1,2</sup> , Atali A. Agakhanov<sup>3</sup>, Elena I. Sandimirova<sup>1</sup>, Anna Vymazalova<sup>4</sup> , Valery M. Chubarov<sup>1</sup> and Andrey A. Zolotarev<sup>2</sup> 

<sup>1</sup>Department of Mineralogy, Institute of Volcanology and Seismology FEB RAS, 9 Piiipa boulevard, Petropavlovsk-Kamchatsky, Kamchatsky Krai, 683006, Russia; <sup>2</sup>St. Petersburg State University, University emb., 7/9, St. Petersburg, 199034, Russia; <sup>3</sup>Fersman Mineralogical Museum of the Russian Academy of Sciences, Leninsky Prospekt 18-2, 119071 Moscow, Russia; and <sup>4</sup>Czech Geological Survey, Geologická 6, 152 00 Prague 5, Czech Republic

### Abstract

Kufahrite, PtPb, is a new mineral (IMA2020-045) from the Ledyanoy Creek placer, Koryak Highlands, Russia. The mineral was found in isoferroplatinum (Pt<sub>3</sub>Fe) grains extracted from a heavy-mineral concentrate, together with tetraferroplatinum (PtFe), tulameenite (Pt<sub>2</sub>FeCu), native iridium, hollingworthite (RhAsS) and Cr-rich spinel. Kufahrite occurs as part of alteration rims which are formed together with tetraferroplatinum after isoferroplatinum, or as grains up to 150 μm in size. According to powder X-ray diffraction analyses kufahrite is isotypic to its synthetic analogue, it is hexagonal and crystallises in space group  $P6_3/mmc$  adopting the nickeline structure type. Its unit-cell parameters are:  $a = 4.2492(6)$  Å;  $c = 5.486(6)$  Å;  $V = 85.78$  Å<sup>3</sup> and  $Z = 2$ . The calculated density is 14.80 g/cm<sup>-3</sup>. The strongest diffraction lines are [ $d$ , Å ( $I$ , %) ( $hkl$ )]: 3.052 (80) (101), 2.197 (100) (102), 2.125 (28) (110), 1.747 (18) (210), 1.528 (35) (202), 1.240 (18) (212) and 0.958 (22) (312). The Vickers hardness is 295 kg/mm<sup>2</sup> (range 262–320,  $n = 5$ ), corresponding to a Mohs hardness of 4. The empirical formula of kufahrite, calculated from a mean value of 23 electron-microprobe analyses is (Pt<sub>0.94</sub>Rh<sub>0.04</sub>)Σ<sub>0.98</sub>(Pb<sub>0.83</sub>Sb<sub>0.19</sub>)Σ<sub>1.02</sub>. The name (pronounced as [ku fa rait]) honours Fahrid Shakirovitch Kutuyev (1943–1993), a geologist from the Institute of Volcanology of USSR Academy of Sciences, who played a key role in the discovery of the Koryak–Kamchatka Platinum Belt, including the Ledyanoy Creek placer platinum deposit, where the new mineral has been discovered.

**Keywords:** new mineral, platinum, lead, alloy, ultramafic, placer, Ural–Alaskan type, Galmoenan, PtPb, Kamchatka

(Received 8 November 2020; accepted 22 February 2021; Accepted Manuscript published online: 26 February 2021; Associate Editor: Oleg I Siidra)

### Introduction

A very limited number of alloys of platinum-group elements (PGE) and Pb are known as approved mineral species and these are all Pd–Pb alloys, such as zvyagintsevite, Pd<sub>3</sub>Pb; plumbopalladinite, Pd<sub>3</sub>Pb<sub>2</sub>; and norilskite, (Pd,Ag)<sub>7</sub>Pb<sub>2</sub>. These minerals are normally described in Cu–Ni–PGE deposits and allocated to the latest mineralisation stages of low- $T$  evolved sulfide liquids (Tolstykh *et al.*, 2020) or post-magmatic fluids (Spiridonov *et al.*, 2015; Ames *et al.*, 2017). Platinum and Pb have been reported previously constituting the sulfide and selenide phases (e.g. inaglyite, Cu<sub>3</sub>Pb(Ir,Pt)<sub>8</sub>S<sub>16</sub> and crerarite, Pt<sub>2-x</sub>(Bi,Pb)<sub>11</sub>(S,Se)<sub>11</sub>), but Pt–Pb alloys remained unknown.

This paper describes the first Pt–Pb intermetallic phase – the new mineral kufahrite, PtPb, which has a synthetic analogue but has never been described previously in Nature. The new mineral was found during panning at the Ledyanoy Creek placer (61°00'N, 166°05'E) related to the Galmoenan Ural–Alaskan type

ultramafic complex at the Koryak Highlands, Far East Russia (Fig. 1). Kufahrite (Cyrillic: куфарит) is named in honour of Fahrid Shakirovitch Kutuyev (1943–1993), a geologist from the Institute of Volcanology of USSR Academy of Sciences, who played a key role in the discovery of the Koryak–Kamchatka platinum belt, including the Ledyanoy placer platinum deposit where the new mineral has been discovered. The holotype material (polished section) is deposited in the Fersman Mineralogical Museum, Moscow, Russia, catalogue No. 5576/1.

The mineral and its name have been approved by the International Mineralogical Association Commission on New Minerals, Nomenclature and Classification (IMA2020-045, Sidorov *et al.*, 2020).

### Occurrence

Kufahrite was found in the heavy-mineral concentrate from Ledyanoy Creek placer, related to the Galmoenan Ural–Alaskan type ultramafic complex, located in the Koryak Highlands, Far East Russia (Fig. 1). Ledyanoy Creek placer together with Levtyrinvyayam Creek placer produced more than 60 metric tons of platinum during 1994–2012 (Nazimova *et al.*, 2011; Sidorov *et al.*, 2012), which makes them one of the largest platinum-group mineral (PGM) placers worldwide. The Galmoenan complex comprises a dunite core surrounded by a rim grading outwards

†Sadly, since this paper was accepted the first author, Evgeniy G. Sidorov, has passed away.

\*Author for correspondence: Anton V. Kutuyev, Email: [anton.v.kutuyev@gmail.com](mailto:anton.v.kutuyev@gmail.com)

Cite this article: Sidorov E.G., Kutuyev A.V., Zhitova E.S., Agakhanov A.A., Sandimirova E.I., Vymazalova A., Chubarov V.M. and Zolotarev A.A. (2021) Kufahrite, PtPb, a new mineral from Ledyanoy Creek placer, Galmoenan ultramafic complex, Koryak Highlands, Russia. *Mineralogical Magazine* 85, 254–261. <https://doi.org/10.1180/mgm.2021.18>

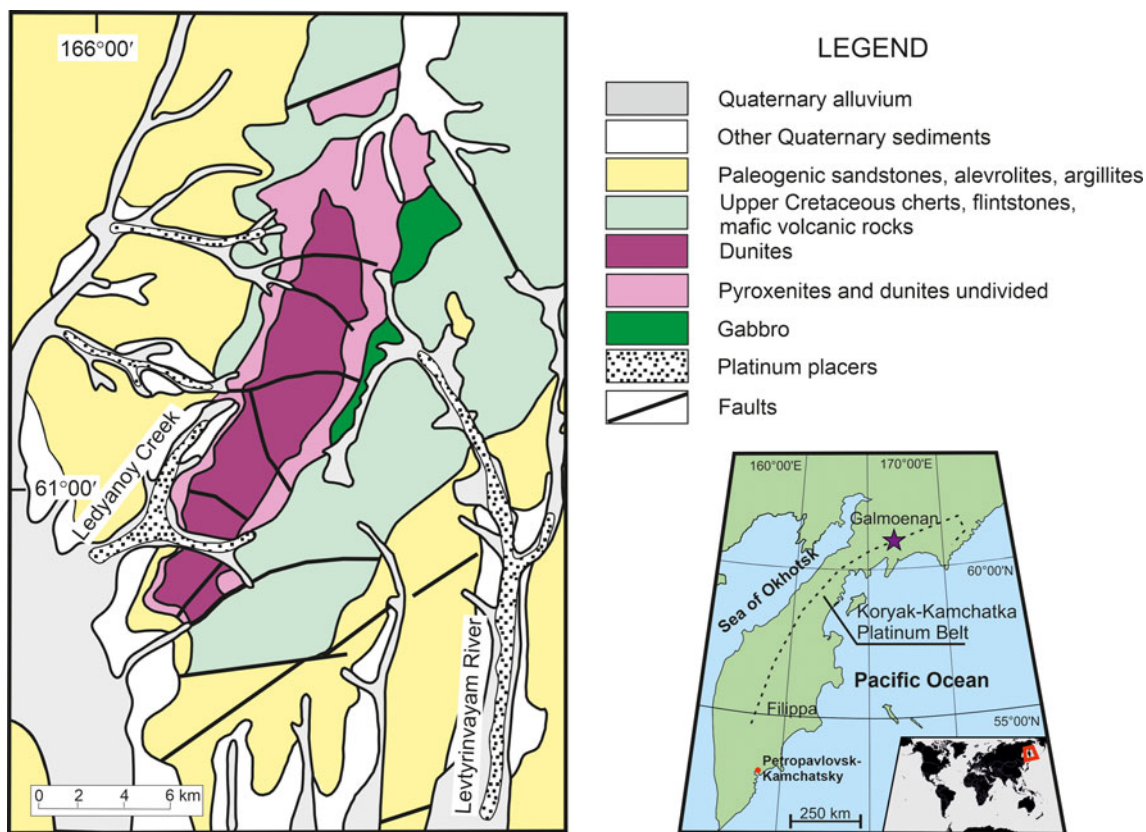


Fig. 1. The position and structure of the Galmoenan complex and Ledyanoy Creek placer. Modified from Astrakhantsev *et al.* (1991).

of wehrlite, clinopyroxenite and gabbro units, which is typical of the Ural–Alaskan type (Fig. 1, Astrakhantsev *et al.*, 1991; Batanova *et al.*, 1994, 2005). The majority of the platinum is concentrated in chromitites, located at the dunite unit of the complex (Mochalov and Bortnikov, 2008; Nazimova *et al.*, 2011; Sidorov *et al.*, 2012). The prevailing PGM is isoferroplatinum  $Pt_3Fe$ , associated with native osmium, native iridium, tetraferroplatinum  $PtFe$ , tulameenite  $Pt_2FeCu$ , laurite  $RuS_2$ , irarsite  $IrAsS$ , and numerous less abundant minerals (Tolstykh *et al.*, 2004; Sidorov *et al.*, 2012). Ledyanoy Creek placer is located at the southwestern margin of the Galmoenan complex, in close proximity of the dunite outcrops (Fig. 1). The placer assemblage is nearly identical to those of the lode chromitites, giving evidence of the latter being the primary source of the PGM (Tolstykh *et al.*, 2004).

Kufahrite occurs as a constituent of tetraferroplatinum and tulameenite rims after isoferroplatinum (Fig. 2a–d). In one case, it together with hollingworthite overgrows native iridium crystals enclosed in the tulameenite rim over isoferroplatinum (Fig. 2d). The width of kufahrite rims or size of its grains normally does not exceed  $10\mu m$  (Fig. 2a,b,d), and only one grain  $150\times 100\mu m$  was observed (Fig. 2c). Along with the minerals listed above, kufahrite is associated with Cr-rich spinel, native iridium and hollingworthite (Fig. 2a–d). A similar mineral assemblage is present in the partly serpentinised chromitites of the Galmoenan complex (Fig. 2e,f).

### Physical and optical properties

Kufahrite is opaque and has a metallic lustre. Its colour is white; streak was not observed because of the tiny size of the grains and

paucity of material. Micro-indentation measurements yielded a mean value of  $295\text{ kg/mm}^2$  (VHN range: 262–320,  $n=5$ ), which corresponds to a Mohs hardness of 4. The mineral is malleable, and other physical properties, such as cleavage, parting and fracture, were not observed. Its density could not be measured due to the small grain size and their occurrence in intergrowths with isoferroplatinum, tulameenite and other minerals (Fig. 2). The mineral density, calculated using the unit-cell dimensions, is  $14.80\text{ g/cm}^3$ .

The optical properties of kufahrite in reflected light are as follows: white colour, strong bireflectance,  $\Delta R=5.03\%$  (589 nm); pleochroism is weak, from white to greyish-white; anisotropy is moderate, rotation tints vary from light brown to grey, and internal reflections are not observed. Reflectance values, measured in air with SiC reference material, are listed in Table 1 and plotted in Fig. 3.

### Chemical composition

Electron microprobe analyses ( $n=23$ ) were obtained in EDS mode (15 kV accelerating voltage and 0.7 nA beam current with beam diameter 0.2 nm) using a Tescan Vega-3 electron microscope equipped with an Oxford X-Max 80 detector and gave contents of Pt, Pb, Sb and Rh (Tables 2, 3). The contents of other elements with an atomic number higher than carbon are below detection limits. The contents of Sb and Rh are below the limits of detection in some grains, but may reach 3.69 and 12.84 wt.% respectively in the others. The empirical formula calculated on the basis of 2 atoms per formula unit is:  $(Pt_{0.94}Rh_{0.04})_{\Sigma 0.98}(Pb_{0.83}Sb_{0.19})_{\Sigma 1.02}$ . The simplified formula is Pt

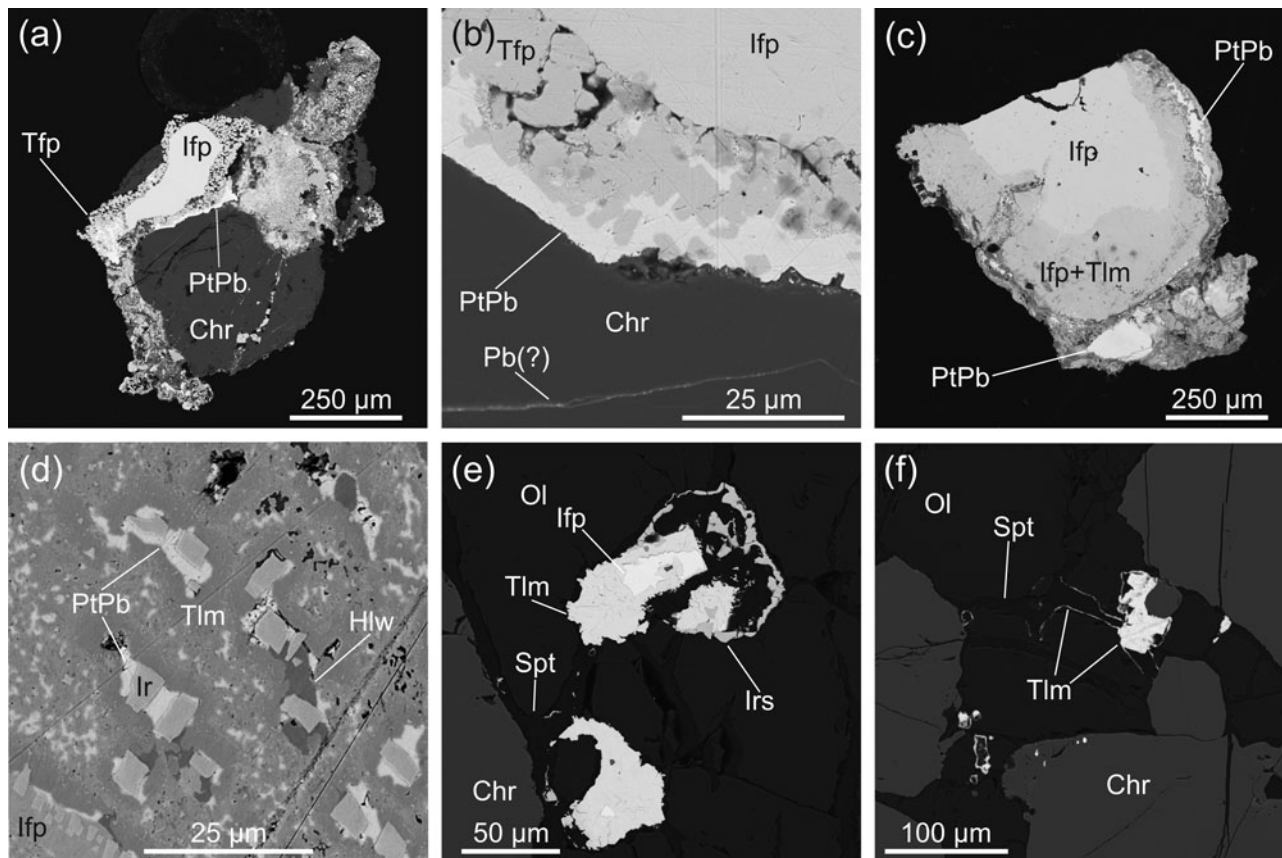


**Fig. 2.** Kufahrite (PtPb) and associated minerals from Ledyanoy Creek placer. (a) Thin rim of kufahrite and tetraferroplatinum (Tfp) over isoferroplatinum (Ifp) at the contact with chromite (Chr); (b) close-up of Fig. 1a; (c) relatively large kufahrite grain associated with isoferroplatinum and tulameenite (Tlm), holotype material sample No 5576/1 stored in the Fersman Mineralogical Museum; (d) intergrowths of kufahrite and hollingworthite (Hlw) with native iridium (Ir) as inclusions in metasomatic tulameenite rim over isoferroplatinum; (e, f) polished samples from the Galmoenan complex which represent the textural position of minerals analogous to those coexisting with kufahrite, note that tulameenite and irarsite (Irs) fringe the walls of serpentine veinlets, indicating late origin of these PGM. Polished section, back-scattered electron images.

(Pb,Sb). The ideal composition is PtPb, which requires Pt 48.49, Pb 51.51, total 100 wt.%. There is a linear negative correlation between Pb and Sb content in kufahrite (Fig. 4) indicating that these elements occur at one crystallographic site.

### Crystal structure

The structure refinement based on single-crystal X-ray diffraction data could not be carried out because of the absence of a crystal of suitable quality and general paucity of available material. The data were collected from one available grain ( $\sim 70 \mu\text{m}$ ) extracted from the polished block (Fig. 2c) that has been previously analysed by electron-microprobe analyses. The grain has been examined for full data collection in the air at room temperature using a Bruker SMART APEX single-crystal diffractometer operated at 50 kV, 40 mA and equipped with a CCD area detector and graphite-monochromated  $\text{MoK}\alpha$  radiation ( $\text{MoK}\alpha$ ,  $\lambda = 0.71073 \text{ \AA}$ ). Later the same crystal was subjected to full data collection by a more powerful machine – Bruker Apex II Duo diffractometer ( $\text{MoK}\alpha$  radiation) operated at 50 kV, 40 mA and equipped with a CCD area detector. The intensity data were reduced and corrected for Lorentz, polarisation and background effects using Bruker software *Apex2* (Bruker AXS, 2014). The data analyses showed that only  $\sim 15\%$  of reflections can be indexed within the following unit cell (showing the best match): symmetry hexagonal,  $a = 4.209(3) \text{ \AA}$ ,  $c = 5.476(13) \text{ \AA}$ ,  $V = 84.0(2) \text{ \AA}^3$  because the studied grain

represents a multicomponent twin. In both cases the data allowed only an estimation of the unit-cell parameters without any further satisfactory data processing. Poor data quality is also partly due to high absorbency of Pb. The reciprocal space slices (obtained by processing the data using *CrysAlis PRO*, Agilent Technologies, 2014) reconstructed for data processed using the aforementioned unit cell are shown in Fig. 5 from which it is evident that reflections that do not suit the unit cell occur randomly excluding their appearance due to a superstructure.

Powder X-ray diffraction (XRD) data were collected with a Rigaku R-axis Rapid II diffractometer (Debye–Scherrer geometry,  $d = 127.4 \text{ mm}$ ) equipped with a rotating anode X-ray source ( $\text{CoK}\alpha$ ,  $\lambda = 1.79021 \text{ \AA}$ ) and a curved image plate detector. The data were collected for 600 seconds from the same small grain ( $\sim 70 \mu\text{m}$ ) extracted from the polished block (Fig. 2c) that was analysed previously by electron-microprobe analyses. The same grain as used for single-crystal X-ray diffraction was studied with no additional treatment. The data were recorded from the grain rotating around the  $\omega$  axis. The data were integrated using the software package *Osc2Tab/SQRay* (Britvin et al., 2017). The obtained powder XRD pattern (Fig. 6) of kufahrite is very close to that reported in the JCPDS-ICDD database, # 01-077-3195 (powder diffraction files from the International Centre for Diffraction Data, <https://www.icdd.com/>), which corresponds to the synthetic phase PtPb (Zhuravlev et al., 1962). Table 3 represents a comparison of the powder X-ray diffraction pattern of a



**Table 1.** Reflectance data for kufahrite\*.

$\lambda$ (nm)	$R_{min}$	$R_{max}$	$\lambda$ (nm)	$R_{min}$	$R_{max}$
400	46.36	49.17	560	53.69	58.41
420	45.66	48.26	580	54.99	59.91
440	45.84	47.72	<b>589</b>	<b>55.56</b>	<b>60.59</b>
460	46.35	49.52	600	56.37	61.41
<b>470</b>	<b>47.11</b>	<b>50.26</b>	620	57.31	62.05
480	47.51	51.05	640	57.94	63.08
500	49.18	52.98	<b>650</b>	<b>57.73</b>	<b>63.27</b>
520	50.44	54.76	660	58.23	63.26
540	51.51	56.79	680	58.27	63.63
<b>546</b>	<b>52.73</b>	<b>57.14</b>	700	58.30	63.86

\*Reflectance data are plotted in Fig. 3; data for wavelengths recommended by the IMA Commission on ore microscopy (COM) are marked in boldtype.

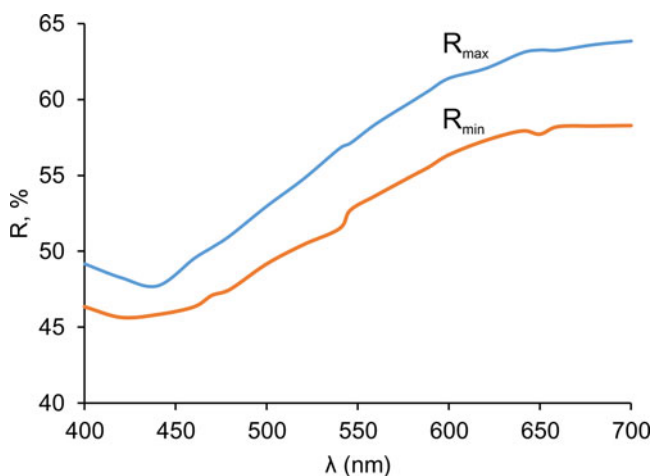


**Fig. 3.** Reflectance data for kufahrite in air. Blue line –  $R_{max}$  and orange line –  $R_{min}$ .

grain of kufahrite and synthetic PtPb. As it is evident from the table, both powder patterns show a satisfactory agreement in reflection positions and intensities. Nevertheless, due to the paucity of available material, the kufahrite diffraction pattern is characterised by considerable low intensities.

The crystal structure of kufahrite was impossible to refine using (1) single-crystal or (2) powder X-ray diffraction data due to (1) absence of single crystals and (2) paucity of available material, low reflection intensities and the fact that atoms are located in the special positions (see below). The crystal structure of the PtPb synthetic compound was described by Zhuravlev *et al.* (1962), and has the NiAs structure type (Fig. 7a). In the NiAs structure type both atoms occupy special positions: Ni (0, 0, 0) (denoted here as the A site) and As ( $\frac{1}{3}$ ,  $\frac{2}{3}$ ,  $\frac{1}{4}$ ) (denoted here as the B site). The A site is octahedrally coordinated, whereas the B site is located within trigonal prism (Fig. 7b,c). In our case, the experimentally obtained powder pattern has been indexed in the  $P6_3/mmc$  space group using the structure data for the synthetic PtPb compound (Fig. 6, Table 3) and showed good agreement in reflection positions and intensities. It is worth noting that the NiAs structure type is widespread for minerals of the nickeline group to which kufahrite belongs. Experimental data do not allow distinguishing whether Pt and Pb are ordered or disordered in the A and B sites of the crystal structure. This is because the crystal chemical formulas of ordered ( $Pt_{0.95}Rh_{0.05}(Pb_{0.80}Sb_{0.20})$ ) (A site = 76 electrons per formula unit and B site = 76 epfu) and disordered, e.g. ( $Pt_{0.6}Pb_{0.3}Sb_{0.1}(Pb_{0.5}Pt_{0.4}Sb_{0.1})$ ) (A site = 76 epfu and

**Table 2.** Chemical data (in wt.%) ( $n = 23$ ) for kufahrite

Constituent	Mean	Range	S.D.	Reference material
Pt	47.51	46.31–48.84	0.82	Pt
Pb	45.41	36.83–54.13	6.36	PbTe
Sb	6.03	b.d.l.–12.84	5.08	Sb
Rh	1.21	b.d.l.–3.69	1.22	Rh
Total	100.16			

S.D. – standard deviation; b.d.l. – below detection limit

**Table 3.** Powder X-ray diffraction data for kufahrite and its synthetic analogue.

Kufahrite (this study)					Synthetic analogue of kufahrite* (Zhuravlev <i>et al.</i> , 1962)	
$l_{meas}$	$d_{meas}$ (Å)	$h$	$k$	$l$	$l_{meas}$	$d_{meas}$ (Å)
<b>80</b>	<b>3.052</b>	<b>1</b>	<b>0</b>	<b>1</b>	<b>82</b>	<b>3.059</b>
8	2.743	0	0	2	<1	2.735
<b>100</b>	<b>2.197</b>	<b>1</b>	<b>0</b>	<b>2</b>	<b>100</b>	<b>2.197</b>
<b>28**</b>	<b>2.125</b>	<b>1</b>	<b>1</b>	<b>0</b>	<b>78</b>	<b>2.130</b>
4	1.843	2	0	0	4	1.844
<b>18</b>	<b>1.747</b>	<b>2</b>	<b>0</b>	<b>1</b>	<b>14</b>	<b>1.748</b>
3	1.682	1	1	2	<1	1.680
4	1.636	1	0	3	10	1.635
<b>35</b>	<b>1.528</b>	<b>2</b>	<b>0</b>	<b>2</b>	<b>27</b>	<b>1.529</b>
3	1.393	2	1	0	2	1.394
3	1.367	0	0	4	5	1.368
14	1.350	2	1	1	10	1.351
10	1.297	2	0	3	4	1.297
3	1.286	1	0	4	2	1.282
<b>18</b>	<b>1.240</b>	<b>2</b>	<b>1</b>	<b>2</b>	<b>22</b>	<b>1.242</b>
9	1.151	1	1	4	14	1.151
2	1.124	3	0	2	<1	1.122
11	1.108	2	1	3	4	1.108
4	1.099	2	0	4	1	1.098
11	1.062	2	2	0	5	1.065
2	1.050	1	0	5	2	1.049
6	1.006	3	1	1	3	1.006
3	0.976	2	1	4	1	0.976
<b>22**</b>	<b>0.958</b>	<b>3</b>	<b>1</b>	<b>2</b>	<b>1</b>	<b>0.958</b>

\*JCPDS-ICDD database, card # 01-077-3195. The strongest lines are given in bold. Note: synthetic PtPb was prepared by smelting of lead and platinum (99.9 wt.%) in a resistance oven (Zhuravlev *et al.*, 1962).

\*\*The difference of intensities between measured and calculated powder patterns for 110 and 312 reflections can be caused by the fact that a solid grain has been used coupled with the geometry of the diffractometer which imply rotation around the  $\omega$  axis. These two factors can cause a textured effect on the sample and changes in measured reflection intensities.

B site = 77 epfu) modifications are nearly identical in the number of electrons, though the low intensity of reflections does not allow the scattering power to be determined with high accuracy. A rough comparison of observed and calculated powder diffraction data taken from a model with different occupation on the A and B sites shows agreement with the experimental chemical formula. At the same time, the chemical data allow clear discrimination of the phase under study from the approved mineral species. The modelling of theoretical powder diffraction patterns using the Vesta program (Momma and Izumi, 2011) showed that different variants in the site occupancies (calculated for modifications with different distribution of Pb, Sb, Pt and Rh using aforementioned occupancies) do not lead to significant changes in the intensity of reflections (Supplementary Table S1, see below).

The chemical data show a negative linear correlation between Pb and Sb content (Fig. 4), such a correlation is absent for Pt and Sb

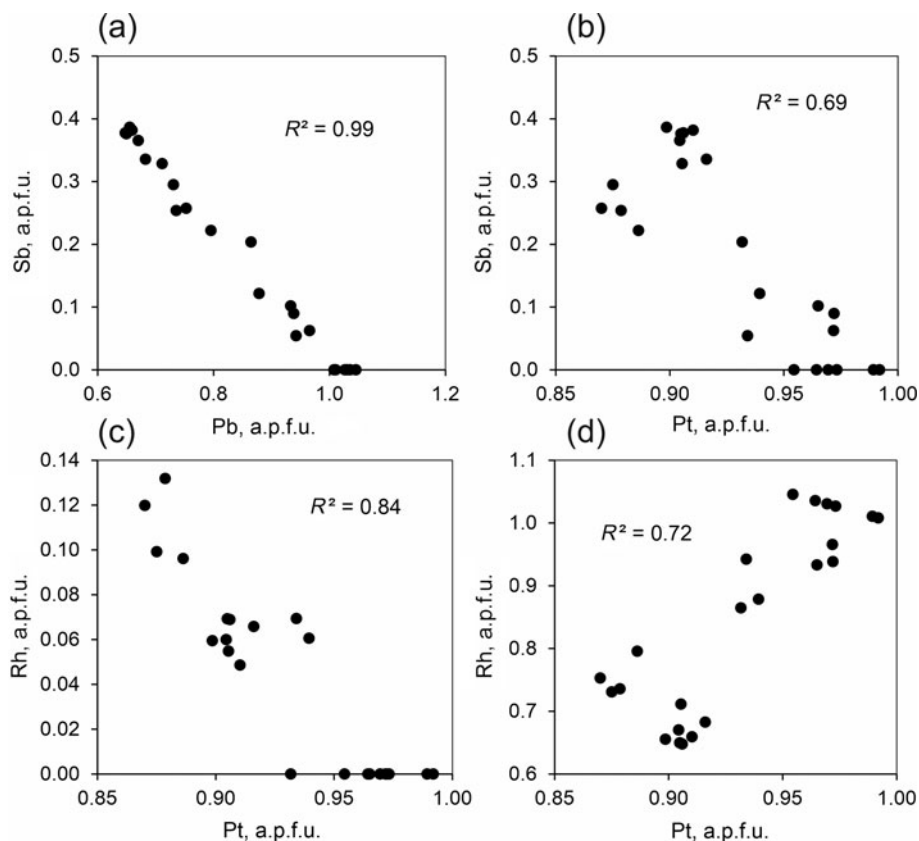


**Fig. 4.** Element correlation for kufahrite. Note the excellent ( $R^2 = 0.99$ ) Pb vs. Sb and good ( $R^2 = 0.84$ ) Pt vs. Rh negative correlations that point to Pb and Sb occurring at one crystallographic site, while Pt and Ru occupy the other site.

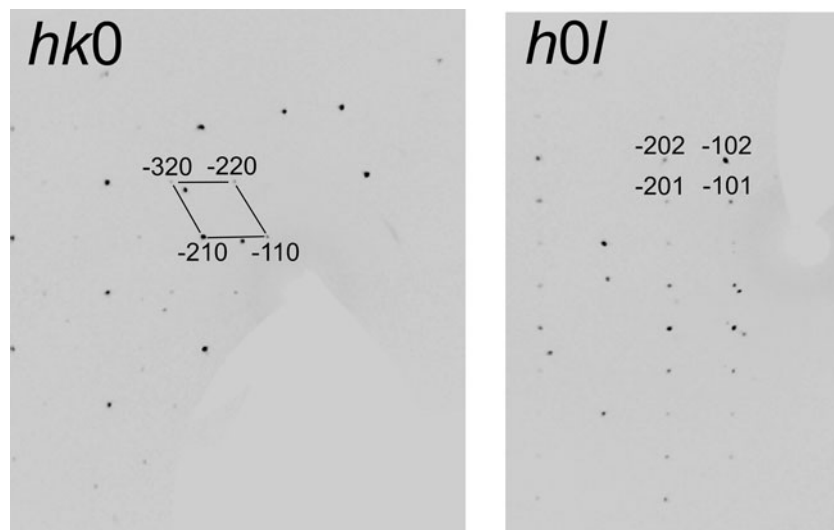


**Fig. 5.** Slices of reciprocal space of kufahrite.

(Fig. 4b), whereas Pt shows some correlation with Rh (Fig. 4c). It is worth noting that the experimental work of Zhuravlev and co-authors (1962) has shown the existence of a solid-solution series for PtBi–PtSb and PtBi–PtPb, which indicates the potential substitution of Pb by Sb. Considering all of the above, we can assume that Pb and Sb occur at one crystallographic site, while Pt and Rh occupy another crystallographic site. Moreover, Pb has been reported as an admixture in stumpflite PtSb (Melcher and Lodziak, 2007) which also indirectly confirms the presence of solid solutions series

PtPb–PtSb. By analogy with other nickeline-group minerals, we can suggest that for kufahrite Pt (and possibly Rh admixture) occurs at the A site, whereas the Pb and Sb admixture occupies the B site (Fig. 7). This is evident by the fact that for other nickeline-group minerals with the NiAs structure type (1) Pt is found in the A site for stumpflite and (2) Sb occurs in the B site for stumpflite, sudburyite and breithauptite. The comparison of the strongest lines in the powder XRD pattern for kufahrite, its synthetic analogue, stumpflite and sudburyite are shown in Table 4.

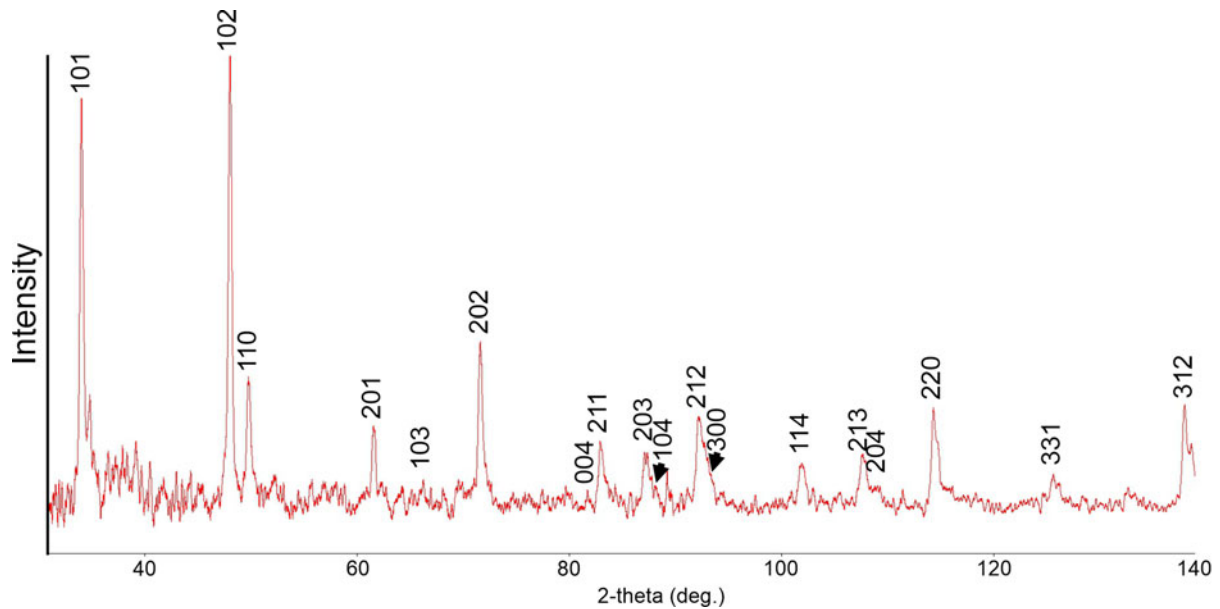


Fig. 6. Experimentally obtained powder XRD pattern with indexed reflections that belong to kufahrte.

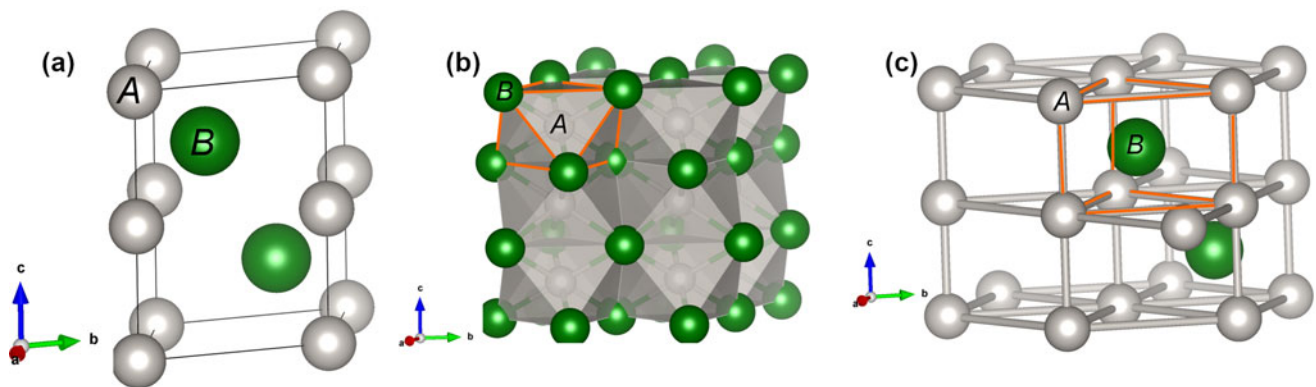


Fig. 7. The NiAs structure type (a); the octahedral coordination of the A site (b); and site B located in a trigonal prism (c).

Table 4. Comparative data of kufahrte, its synthetic analogue, and closely related nickeline-group minerals: stumpflite and sudburyite.

	Kufahrte	Synthetic PtPb	Stumpflite	Sudburyite
Formula	PtPb	PtPb	PtSb	PdSb
Crystal system	Hexagonal	Hexagonal	Hexagonal	Hexagonal
Space group	$P6_3/mmc$	$P6_3/mmc$	$P6_3/mmc$	$P6_3/mmc$
<i>a</i> (Å)	4.2492(6)	4.260	4.175	4.078
<i>c</i> (Å)	5.486(6)	5.470	5.504	5.588
<i>V</i> (Å <sup>3</sup> )	85.78	85.97	83.08	80.48
Calculated density (g/cm <sup>3</sup> )	14.75	15.54	13.61	9.42
The strongest lines in the powder XRD pattern:	3.052 (80), 2.197 (100), 2.125 (28), 1.747 (18), 1.528 (35), 1.240 (18), 0.958 (22)	3.059 (82)*, 2.197 (100), 2.130 (78), 1.748 (14), 1.529 (27), 1.242 (22), 1.151 (14)	3.620 (60)**, 3.030 (100), 2.192 (100), 2.088 (80), 1.720 (40), 1.512 (50), 1.149 (50)	2.980 (70)***, 2.180 (100), 2.030 (70), 1.489 (60), 1.202 (80), 1.152 (60), 0.901 (70)
Reference	This study	Zhuravlev <i>et al.</i> (1962)	Johan and Picot (1972)	Cabri and Laflamme (1974)

\*JCPDS-ICDD database, card # 01-077-3195; \*\*JCPDS-ICDD database, card # 00-025-1482; \*\*\*JCPDS-ICDD database, card # 00-026-0888.

## Relation to other species

Kufahrite fits the 2.CC group according to the Nickel and Strunz classification and the nickeline group of Dana Classification (02.08.11). The new mineral is the natural analogue of synthetic PtPb (Zhuravlev *et al.*, 1962). Kufahrite is also chemically related and isotypic to such nickeline-group minerals as stumpflite, PtSb, (Johan and Picot, 1972) and sudburyite, PdSb, (Cabri and Laflamme, 1974). The comparison of kufahrite, synthetic PtPb, stumpflite and sudburyite is given in Table 4. No mineral close to kufahrite is present in the lists of both valid and invalid unnamed species.

## Genetic implications

Kufahrite has been found as a part of tetraferroplatinum and tulameenite rims after isoferroplatinum (Fig. 2). The origin of tetraferroplatinum and tulameenite rims has been assigned previously to relatively low-temperature alteration processes, which occurred under relatively low  $f_{S_2}$  (Nixon *et al.*, 1990; Cabri and Genkin, 1991; Tolstykh *et al.*, 2004, 2011, 2015; O'Driscoll and González-Jiménez 2016). The main evidence for this conclusion are: (1) the occurrence of both tetraferroplatinum and tulameenite as rims over isoferroplatinum grains (Fig. 2; Nixon *et al.*, 1990; Tolstykh *et al.*, 2004, 2015; Stepanov *et al.*, 2019, 2020); and (2) the presence of these minerals as separate phases in serpentine veinlets (Fig. 2e,f); and (3) experimental studies which proved the possibility of formation of Pt–Fe alloys under hydrothermal conditions (Evstigneeva and Tarkian, 1996). Usually, such reduced hydrothermal conditions are assigned to be a result of a serpentinisation process. Therefore, the possible temperature of kufahrite formation estimated as the temperature of dunite serpentinisation should be below 450°C (Fruh-Green *et al.*, 2004; Klein and Bach, 2009; Evans *et al.*, 2013), or even less than 350°C according to other estimations (Popov *et al.*, 2006).

As stumpflite PtSb and numerous Pd–Pb alloys are related to kufahrite in terms of either crystal structure or composition, it would be fruitful to compare the conditions of their formation with those proposed for kufahrite. Stumpflite was described in the dunite pipe Driekop, one of the several zoned dunite pipes crosscutting the layered sequence of the Bushveld complex (Johan and Picot, 1972). Subsequent studies revealed that this mineral, together with the whole assemblage of Pt–Pd–Sb–Bi–Te–Sn minerals, belong to the latter low-temperature hydrothermal stage (Rudashevsky *et al.*, 1992; Melcher and Lodziak, 2007). In Ural–Alaskan type complexes, stumpflite is an exceptionally rare mineral. The only available description is of those from the Filippa complex, Kamchatka, where it occurs as a part of metasomatic sperrylite rim after isoferroplatinum (Sidorov *et al.*, 2004). Therefore, stumpflite of both layered intrusions and Ural–Alaskan type complexes may be assigned to the post-magmatic overprint in the same way that was proposed for kufahrite.

Palladium–lead alloys are also the minerals with an affinity to layered intrusions (e.g. Cabri, 2002). The most common of them, zvyagentsevit Pd<sub>3</sub>Pb and plumbopalladinite Pd<sub>3</sub>Pb<sub>2</sub>, were first reported in the deposits of the Norilsk group, where their origin has been assigned to post-magmatic processes (e.g. Spiridonov *et al.*, 2015). The only description of Pd–Pb minerals in Ural–Alaskan type complexes is those of zvyagentsevit in the altered parts of isoferroplatinum grains of the Veresovoborsky Complex, Urals (Stepanov *et al.*, 2020). Here its textural position and assemblage irrefutably points towards post-magmatic origin.

Summarising the above, kufahrite, its Sb counterpart stumpflite and Pd–Pb alloys all are the result of post-magmatic processes probably formed from hydrous fluids. Kufahrite extends the wide group of PGE minerals for which hydrothermal origin have been proven.

**Acknowledgements.** We are thankful to Anatoly Kasatkin for his recommendations and fruitful discussion. Members of the CNMNC are greatly acknowledged for their advice and critical remarks during the preparation of the new mineral submission form. This work was largely supported by RFBR grant #20-05-00290. The XRD data were collected using the XRD Resource Center of St. Petersburg State University. Finally, we thank Louis J. Cabri, František Laufek and three anonymous reviewers for their suggestions and Associate Editor Oleg Siidra and Principal Editor Stuart Mills for the manuscript handling.

**Supplementary material.** To view supplementary material for this article, please visit <https://doi.org/10.1180/mgm.2021.18>

## References

- Agilent Technologies (2014) *CrysAlis, PRO*. Agilent Technologies Ltd., Yarnton, UK.
- Ames D.E., Kjarsgaard I.M., McDonald A.M. and Good D.J. (2017) Insights into the extreme PGE enrichment of the W horizon, marathon Cu–Pd deposit, Coldwell alkaline complex, Canada: Platinum-group mineralogy, compositions and genetic implications. *Ore Geology Reviews*, **90**, 723–747.
- Astrakhantsev O.V., Batanova V.G. and Perfil'ev A.S. (1991) The structure of the dunite-clinopyroxenite-gabbro Gal'moenan complex. *Geotectonics*, **25**, 132–144.
- Batanova V.G. and Astrakhantsev O.V. (1994) Island arc mafic-ultramafic plutonic complexes of North Kamchatka. *Proceedings of 29th International Geological Congress*, 129–143.
- Batanova V.G., Pertsev A.N., Kamenetsky V.S., Ariskin A.A., Mochalov A.G. and Sobolev A.V. (2005) Crustal evolution of island-arc ultramafic magma: Galmoenan pyroxenite-dunite plutonic complex, Koryak Highland (Far East Russia). *Journal of Petrology*, **46**, 1345–1366.
- Britvin S.N., Dolivo-Dobrovolsky D.V. and Krzhizhanovskaya M.G. (2017) Software for processing of X-ray powder diffraction data obtained from the curved image plate detector of Rigaku RAXIS Rapid II diffractometer. *Zapiski RMO (Proceedings of the Russian Mineralogical Society)*, **146**, 104–107 [in Russian with English abstract].
- Bruker AXS (2014) *APEX2; Version 2014.11-0*. Bruker AXS: Madison, WI, USA, 2014.
- Cabri L.J. (2002) The platinum-group minerals. Pp. 13–129 in: *The Geology, Geochemistry, Mineralogy and Mineral Beneficiation of Platinum-Group Elements* (L.J. Cabri, editor). CIM Special Volume, **54**. Canadian Institute of Mining, Metallurgy, and Petroleum (CIM), Westmount, QC, Canada.
- Cabri L.J. and Genkin A.D. (1991) Re-examination of Pt alloys from lode and placer deposits, Urals. *The Canadian Mineralogist*, **29**, 419–425.
- Cabri L.J. and Laflamme J.H.G. (1974) Sudburyite, a new palladium-antimony mineral from Sudbury, Ontario. *The Canadian Mineralogist*, **12**, 275–279.
- Evans B.W., Hattori K. and Baronnet A. (2013) Serpentinite: What, why, where? *Elements*, **9**, 99–106.
- Evstigneeva T. and Tarkian M. (1996) Synthesis of platinum-group minerals under hydrothermal conditions. *European Journal of Mineralogy*, **8**, 549–564.
- Fruh-Green G.L., Connolly J.A.D., Plas A., Kelley D.S. and Grobety B. (2004) Serpentinization of oceanic peridotites: Implications for geochemical cycles and biological activity. *Geophysical Monograph Series*, **144**, 119–136.
- Johan Z. and Picot P. (1972) La stumpflite, Pt (Sb,Bi), un nouveau mineral; *Bulletin de la Société française de Minéralogie et de Cristallographie* **95**, 610–613 [in French].
- Klein F. and Bach W. (2009). Fe–Ni–Co–O–S Phase Relations in Peridotite–Seawater Interactions. *Journal of Petrology*, **50**, 37–59.
- Melcher F. and Lodziak J. (2007) Platinum-group minerals of concentrates from the driekop platinum pipe, eastern bushveld complex – tribute to Eugen F. Stumpfl. *Neues Jahrbuch für Mineralogie – Abhandlungen*, **183**, 173–195.

- Mochalov A.G. and Bortnikov N.S. (2008) New criteria of the genesis of platinum group minerals in intergrowths with pyroxenes from zonal gabbro-pyroxenite-dunite massifs in the South Koryak Highland (Russia). *Geology of Ore Deposits*, **421**, 941–945.
- Momma K. and Izumi F. (2011) VESTA 3 for three-dimensional visualization of crystal, volumetric and morphology data. *Journal of Applied Crystallography*, **44**, 1272–1276.
- Nazimova Y.V., Zaytsev V.P. and Petrov S.V. (2011) The Galmoenan massif, Kamchatka, Russia: geology, PGE mineralization, applied mineralogy and beneficiation. *The Canadian Mineralogist*, **49**, 1433–1453.
- Nixon G.T., Cabri L.J. and Laflamme J.H.G. (1990) Platinum-group-element mineralization in lode and placer deposits associated with the Tulameen Alaskan-type complex, British Columbia. *The Canadian Mineralogist*, **28**, 503–535.
- O'Driscoll B. and González-Jiménez J.M. (2016) Petrogenesis of the platinum-group minerals. Pp. 489–578 in: *Highly Siderophile and Strongly Chalcophile Elements in High-Temperature Geochemistry and Cosmochemistry* (J. Harvey and J.M.D. Day, editors). Reviews in Mineralogy and Geochemistry, **81**. Mineralogical Society of America and the Geochemical Society, Chantilly, Virginia, USA.
- Popov K.V., Bazylev B.A. and Shcherbakov V.P. (2006) Temperature range for magnetization of oceanic spinel peridotites. *Oceanology*, **46**, 256–267.
- Rudashevsky N.S., Avdontsev S.N. and Dneprovskaya M.B. (1992) Evolution of PGE mineralization in hortonolitic dunites of the Mooihoek and Onverwacht pipes, Bushveld complex. *Mineralogy and Petrology*, **47**, 37–54.
- Sidorov E.G., Tolstykh N.D., Podlipsky M.Y. and Pakhomov I.O. (2004) Placer PGE minerals from the Filippa clinopyroxenite-dunite massif (Kamchatka). *Geologiya i Geofizika*, **45**, 1128–1144 [in Russian].
- Sidorov E.G., Kozlov A.P. and Tolstykh N.D. (2012) *The Galmoenan Ultrabasic Massif and its Platinum Potential*. Pp. 288. Nauchnyi Mir, Moscow [in Russian].
- Sidorov E.G., Sandimirova E.I., Chubarov V.M. and Ananiev V.V. (2018) Accessory minerals of the mafic-ultramafic massif Galmoenan (Koryakskoye upland, Kamchatka). *Zapiski RMO (Proceedings of the Russian Mineralogical Society)*, **147**, 44–64.
- Sidorov E.G., Kutyrev A.V., Zhitova E.S., Agakhanov A.A., Sandimirova E.I., Vymazalova A. and Chubarov V.M. (2020) Kufahrte, IMA 2020-045. CNMNC Newsletter No. 57. *Mineralogical Magazine*, **84**, 791–794.
- Spiridonov E.M., Kulagov E.A., Serova A.A., Kulikova I.M., Korotaeva N.N., Sereda E.V., Tushentsova I.N., Belyakov S.N. and Zhukov N.N. (2015) Genetic Pd, Pt, Au, Ag, and Rh mineralogy in Noril'sk sulfide ores. *Geology of Ore Deposits*, **57**, 402–432.
- Stepanov S., Palamarchuk R., Kozlov A., Khanin D., Varlamov D. and Kiseleva D. (2019) Platinum-group minerals of Pt-placer deposits associated with the Svetloborsky Ural-Alaskan type massif, Middle Urals, Russia. *Minerals*, **9**, 77.
- Stepanov S.Y., Palamarchuk R.S., Antonov A.V., Kozlov A.V., Varlamov D.A., Khanin D.A. and Zolotarev Jr A.A. (2020) Morphology, composition, and ontogenesis of platinum-group minerals in chromitites of zoned clinopyroxenite-dunite massifs the Middle Urals. *Russian Geology and Geophysics*, **61**, 47–67.
- Tarkian M., Evstigneeva T. and Gorshkov A., 1996. Synthesis of Pt- And Pd-sulphides in low temperature (85°C) solutions buffered by clay minerals and graphite: Preliminary results. *Mineralogy and Petrology*, **58**, 71–78.
- Tolstykh N., Krivenko A., Sidorov E., Laajoki, K. and Podlipsky M. (2002) Ore mineralogy of PGM placers in Siberia and the Russian Far East. *Ore Geology Reviews*, **20**, 1–25.
- Tolstykh N.D., Sidorov E.G. and Kozlov A.P. (2004) Platinum-group minerals in lode and placer deposits associated with the Ural-Alaskan-type Galmoenan Complex, Koryak–Kamchatka Platinum Belt, Russia. *The Canadian Mineralogist*, **42**, 619–630.
- Tolstykh N.D., Telegin Y.M. and Kozlov A.P. (2011) Platinum mineralization of the Svetloborsky and Kamenushinsky massifs (Urals Platinum belt). *Russian Geology and Geophysics*, **52**, 603–619.
- Tolstykh N., Kozlov A. and Telegin Y. (2015) Platinum mineralization of the Svetly Bor and Nizhny Tagil complexes, Ural Platinum Belt. *Ore Geology Review*, **67**, 234–243.
- Tolstykh N., Krivolutskaya N., Safonova I., Shapovalova M., Zhitova L. and Abersteiner A. (2020) Unique Cu-rich sulphide ores of the Southern-2 orebody in the Talnakh intrusion, Noril'sk area (Russia): Geochemistry, mineralogy and conditions of crystallization. *Ore Geology Reviews*, **122**, 103525.
- Zhuravlev N.N., Zhdanov G.S. and Smirnova Ye.M. (1962) Investigation of alloys of ternary alloys on a base of superconductive compounds. *Fiz Met Metalloved*, **13**, 62–70 [in Russian].